Superlattices and Microstructures xxx (2017) 1–5

Contents lists available at ScienceDirect

Superlattices and Microstructures

journal homepage: www.elsevier.com/locate/superlattices

Enhancement of visible light photocatalytic activity over bistructural SnO_2 nanobelts

ARTICLE INFO

Article history:
Available online xxx

Keywords:
Nanoparticles
Semiconductors
Partially crystallized structure
Photocatalytic efficiency
Organic pollutant

ABSTRACT

SnO_2 nanobelts were synthesized by hydrothermal method. The structure and morphology were investigated by XRD, Raman spectra, SEM and TEM. The results revealed that the synthesized SnO_2 nanobelts were covered with amorphous surface. For the photocatalytic efficiency of methylene blue, the none-fully crystallized SnO_2 nanobelts were over four times higher than bulk SnO_2. Moreover, the photo-degradation rate constant with SnO_2 nanobelts as photocatalysts was over six times higher than bulk SnO_2. It was considered that the subtle structure of SnO_2 nanobelts not only lowered the band gap but also improved the transfer of charge carriers and trapping effect of solar light. Furthermore, this strategy of enhancing photocatalytic performance could be extended to the other kinds of metal oxide photocatalyst.

1. Introduction

The worldwide applications of organic dyes were closely associated with daily life [1,2]. They were widely applied to a large variety of industries, but the majority of industrial dyes were toxic and mutagenic [3,4]. Therefore, efficient removal of dyes prior to environmental contamination was a significant issue. Most approach failed to remove dye pollutants owing to the slow reaction, expensive instrument and secondary pollution. Photo-degradation gradually attracted great attention owing to its convenience and applicability. In particularly, semiconductor-based material as photocatalysts had been known as a potential candidate for the removal of dyes [5–7].

Tin oxide (SnO_2), as an *n*-type semiconductor, possess a wide band gap (300 K, $E_g = 3.6$ eV). Furthermore, SnO_2 was rarely absorbed by the human and had little health effects even injecting or inhaling [5]. Thus, it had been intensively used in many anticipated and potential fields including photocatalyst [5–7], alkali metal ion batteries [8], gas sensors [9], optoelectronic devices [10] and so on. As a photocatalyst, doping and SnO_2 based composite were feasible ways to improve its performance [5–7]. However, these methods to some extent increased the cost and complexity for the synthesis of materials. On the other hand, few works had been reported for bare SnO_2 with low dimension as photocatalysis.

In current work, low dimensional SnO_2 nanobelts were synthesized via hydrothermal method. The synthesized SnO_2 nanobelts were systemically investigated by XRD, Raman spectra, SEM, and TEM. The photocatalytic performance of SnO_2 nanobelts was evaluated toward the degradation of methylene blue (abbreviated as MB) under solar light. Bulk SnO_2 was also treated with the same conditions to elucidate the difference between nanobelts and bulk SnO_2.

2. Materials and methods

All chemicals (including Bulk SnO_2) without any further purification were supplied from Beijing Chemical Reagent Co. Ltd with analytical-grade reagents. In a typical procedure, 1.5 mmol $Na_2SnO_3 \cdot 4H_2O$ was added into 20 mL NaOH (0.375 mol/L)

[1] These authors contributed equally to this work.

https://doi.org/10.1016/j.spmi.2017.12.058
0749-6036/

solution with stirring for 10 min. Then 20 mL anhydrous alcohol was dissolved in the mixture to obtain a transparent solution. After stirring for 10 min, the solution was loaded into a 50 mL Teflon-lined autoclave. The autoclave was maintained at 200 °C for 24 h. The product was washed with distilled water and anhydrous alcohol, and finally dried in vacuum oven at 60 °C for 24 h.

The morphology and microstructure were characterized by X-ray diffraction (XRD, Rigaku, D8 advance), Raman spectra (LaBRAM HR800, Jobin-Yvon-Horiba), scanning electron microscopy (SEM, Hitachi, S-4800) and transmission electron microscope (TEM, Hitachi, JEM-2100F). The photocatalytic performance was evaluated by the photo-degradation of MB. 30 mg of samples was dissolved into the aqueous solution of MB with a concentration of 10 mg/L^{-1}. The suspension liquid was stirred in the dark for 2 h to achieve the equilibrium of adsorption-desorption. Then the photocatalytic measurement was carried out with a 500 W Xe vapor lamp as the irradiation source (AM 1.5G filter, ~100 mW/cm^2). At every 30 min, the intermediate solution of MB was separated by centrifugation. The remaining concentration and spectral absorbance were recorded by a spectrophotometer (Shimadzu, UV-2550).

3. Results and discussion

The XRD patterns were shown in Fig. 1a. The observed diffraction confirmed highly crystalline nature with tetragonal rutile structure (JCPDS Card No. 41-1445, space group of P42/mnm, $a = 4.7382$ Å and $c = 3.1871$ Å). No diffraction peaks related with the secondary phase were detected. However, the relative diffraction intensity of bulk SnO_2 was obviously stronger than that of SnO_2 nanobelts. The full width at half maximum (FWHM) of SnO_2 nanobelts was also bigger than that of bulk SnO_2. Taking the above in consideration, it could reach the conclusion that the crystalline degree of SnO_2 nanobelt was lower than bulk SnO_2. Fig. 1b presented the Raman spectra of these two different kinds of samples. Bulk SnO_2 exhibited two distinct peaks. As for SnO_2 nanobelts, it just showed one. The bands located at round 474 cm^{-1} and 635 cm^{-1} were related with the E_g and A_{1g} vibration modes of SnO_2, respectively [11–13]. Besides, the peak around 561 cm^{-1} corresponded to the in-plane oxygen vacancy, indicating the existence of amorphous SnO_2 [14].

The morphology and microstructure of SnO_2 nanobelts was characterized by SEM and TEM. Fig. 2a showed that the achieved zoom was fluffy with large scale nanobelts. The higher magnification SEM in Fig. 2b indicated that the nanobelts were crimped and irregular with the length. Moreover, nanobelts were around 200 nm in width and 30 nm in thickness. Fig. 2c reconfirmed the sample was composed with ultrathin nanobelts. The HRTEM image (Fig. 2d) and SAED pattern (inset in Fig. 2d) depicted the detailed structure of SnO_2 nanobelts. The amorphous structure wrapped around the inner crystalline SnO_2. The d-spacing of 2.642 Å between adjacent lattice planes corresponded to the (101) plane of rutile SnO_2. The SAED pattern included a set of weak diffraction spots and rings due to the amorphous surface and polycrystallinity of inner SnO_2. These results were consistent with the above-mentioned XRD patterns and Raman spectra. The diffraction spots were corresponding to the (200), (211) and (321) planes of rutile SnO_2.

Fig. 3a showed the degradation of MB under solar light with SnO_2 nanobelts. The peaks between 600 nm and 700 nm corresponded to the absorption of the heteropoly aromatic linkage [6,7]. The relative intensity of the peak located at 663.5 nm decreased rapidly, indicating the high photocatalytic activity. The normalized concentration (C/C_0) versus irradiation time plotted in Fig. 3b was derived from the UV-vis spectra of MB solution in Fig. 3a according to equation (1):

$$C/C_0 = I/I_0 \tag{1}$$

Herein, C and C_0 were instant and initial concentration of MB, respectively. I and I_0 were the instant and initial intensity of UV-vis absorption peak, respectively. After irradiation for 300 min, almost 80% of MB was photo-degraded with SnO_2 nanobelts, exhibiting four times higher than that of bulk SnO_2 (20%). The kinetics process of photo-degradation was shown in Fig. 3c. The

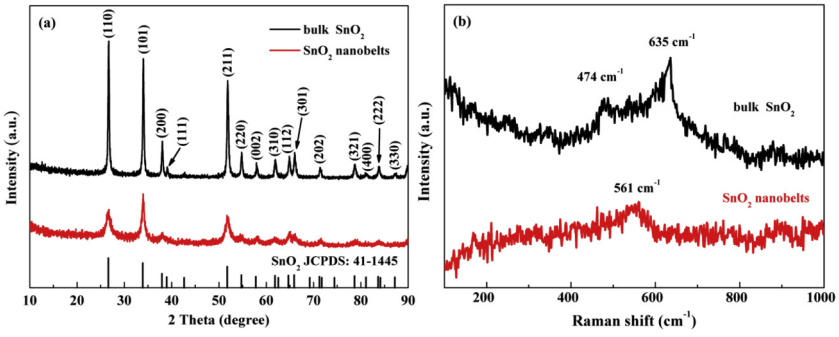

Fig. 1. (a) XRD patterns and (b) Raman spectra of bulk SnO_2 and SnO_2 nanobelts.

Please cite this article in press as: L. Wang, Enhancement of visible light photocatalytic activity over bistructural SnO_2 nanobelts, Superlattices and Microstructures (2017), https://doi.org/10.1016/j.spmi.2017.12.058